# Quantum transport through a multilevel magnetic structure with multiple inelastic scattering in a magnetic field taken into account

Cite as: Low Temp. Phys. **41**, 98 (2015); https://doi.org/10.1063/1.4913204
Published Online: 27 February 2015

V. V. Val'kov, S. V. Aksenov, and E. A. Ulanov

# Quantum transport through a multilevel magnetic structure with multiple inelastic scattering in a magnetic field taken into account

V. V. Val'kov[a] and S. V. Aksenov[b]

*Kirenskii Institute of Physics, Krasnoyarsk 660036, Russia*

E. A. Ulanov

*Siberian Aerospace University, Krasnoyarsk, 660014, Russia*

(Submitted October 6, 2014)
Fiz. Nizk. Temp. **41**, 129–138 (February 2015)

We present a solution for the problem of quantum electron transport through a magnetic atom adsorbed inside a break junction with paramagnetic metal electrodes. In agreement with experimental data, it was assumed that the conduction electrons experience inelastic scattering by the adsorbate due to $s$–$d(f)$-exchange interaction. The Keldysh technique was employed to obtain a general expression describing a current through the multilevel structure at finite temperatures in terms of the nonequilibrium Green's function. The use of the atomic representation allowed to exactly account for the non-equidistant structure of the energy spectrum of a magnetic atom and to simplify substantially the application of the Wick theorem for construction of the nonequilibrium diagrammatic technique for the Hubbard operators. The calculation of the current-voltage characteristics of the magnetic adatom in the tunnel regime at low temperatures revealed the presence of regions with a negative differential conductance in a magnetic field. 
[http://dx.doi.org/10.1063/1.4913204]

## 1. Introduction

Prospects of developing electronic devices operating at the scale of individual atoms and molecules require extensive studies of the kinetic processes in such systems.[1,2] An important role in the electron transport is played by the charge and spin correlations,[3,4] as well as the processes of inelastic scattering at the nano-object with internal degrees of freedom.[5]

Magnetic structures consisting of magnetic atoms or molecules (Mn, Co, Fe, phthalocyanines, etc.) belong to some of the most actively researched systems. These objects are deposited in the region of the break junction between metal electrodes[6–8] or adsorbed on the substrate and probed with a scanning tunneling microscope (STM).[9–11] Experimental studies have shown that the presence of spin-flip processes in inelastic scattering of electrons transported in such systems leads to excitation of the latter.[7,9] As a result, the interaction of atoms and molecules adsorbed onto the surface with the transported particles and external fields allows to implement both stable magnetic and charge states in these systems and provide controlled switching between them.[11,12] This, in particular, makes it possible to design non-volatile magnetic memory devices based on such structures.[13] In addition, due to the dependence of the potential profile on the spin projection of a transported electron, atomic magnetic structures exhibit spin-filtration properties.[14]

The presence of a local environment leads to a dependence of magnetic and, as a result, the transport properties of nanosystems on the geometric structure of the substrate and the location of the adsorbate on it.[15,16] First-principles calculations indicate that the same atomic magnetic structures may exhibit different magnetic properties depending on the substrate on which they are adsorbed.[17–19] A typical example of the anisotropy of the magnetic properties of an adsorbate is the evolution of the Kondo peak in differential conductance upon changing the local environment.[20,21]

This paper presents the development of the theory of quantum transport through a structure of atomic dimension, which takes into account two important factors. The application of atomic statistics[22,23] allowed us not only to modify the method of nonequilibrium Green's functions and formulate the Keldysh diagrammatic technique[24] for a system with multiple interactions (coupling to the contacts, inelastic scattering of conduction electrons by magnetic impurities, and the Coulomb interaction), but also to sum the contributions to the current by all the scattering processes over the parameters of coupling to the contacts. In this approach, we obtained an expression describing the electron current through a multilevel structure with a large number of non-equidistantly spaced transitions at finite temperatures. As a special case, the transport properties of a magnetic adatom in the regime of tunnel coupling and low temperatures were considered. It was shown that allowing for the multiple inelastic scattering leads to a nonequilibrium occupation of the excited states of the system "adatom + electrons," which depends on the applied voltage. It was demonstrated that the negative differential conductivity (NDC) in the current-voltage characteristics (CVC) can arise not only upon changing the magnetic anisotropy parameter of the adatom,[25,26] but also upon switching on a magnetic field.

## 2. The system under study and its Hamiltonian

Let us assume that a magnetic atom with a spin $S = 1$ is adsorbed to the surface in the region between the paramagnetic metal contacts (so-called break junction geometry, see Fig. 1). As a result, due to the spin-orbit interaction with the electrons of the substrate, there arises an anisotropy of the magnetic properties of the adsorbate.[20] Tunneling electron

 

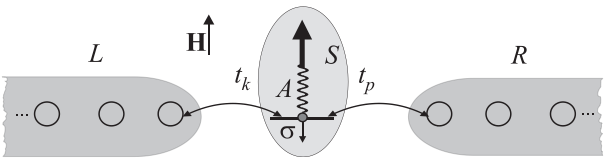


FIG. 1. Magnetic adatom with a spin $S$ located between the metal contacts in an external magnetic field **H**.

transport through such a system is considered in the presence of an external magnetic field **H**.

The Hamiltonian of the system can be written as

$$\hat{H} = \hat{H}_L + \hat{H}_D + \hat{H}_R + \hat{T} + \hat{V}_\varphi. \tag{1}$$

The operators $\hat{H}_L$ and $\hat{H}_R$ in Eq. (1) describe the conduction electrons in the left and right metallic contacts, respectively,

$$\hat{H}_L = \sum_{k\sigma} \xi_{Lk\sigma} c^+_{k\sigma} c_{k\sigma}, \quad \hat{H}_R = \sum_{p\sigma} \xi_{Rp\sigma} d^+_{p\sigma} d_{p\sigma}, \tag{2}$$

where $c^+_{k\sigma}(d^+_{p\sigma})$ is the electron creation operator in the left (right) contact with the wave vector $k(p)$ and spin projection $\sigma$; $\xi_{L(R)k\sigma} = \varepsilon_{L(R)k} - \sigma g_e \mu_B H - \mu$ is the one-electron energy in the left (right) contact, which is referenced to the chemical potential $\mu$ and takes into account the influence of a magnetic field on the electron with the spin projection $\sigma = \pm 1/2$; $g_e$ is the electron $g$-factor in contacts, $\mu_B$ is the Bohr magneton. For the below description of the transport properties of a magnetic adatom, it is important that the contacts are assumed to be fabricated of a single-band metal with the band width $W = 4|t| \sim 1$ eV (where $t$ is the overlap integral of the electron wave functions at the neighboring nodes in contacts), which largely exceeds the characteristic energy parameters of the system.

The central region (region of the device), where the magnetic object is located, is described by the term $\hat{H}_D$:

$$\hat{H}_D = \sum_\sigma \xi_{d\sigma} n_\sigma + U n_\uparrow n_\downarrow + D(S^z)^2 - S^z g \mu_B H + A(\boldsymbol{\sigma}\mathbf{S}), \tag{3}$$

where $\xi_{d\sigma} = \varepsilon_d - \sigma g_e \mu_B H - \mu$ is the spin-dependent energy (referenced to the chemical potential) of an electron located on the outer orbital of the adsorbed atom in an external magnetic field $H$; $\varepsilon_d$ is the one-electron energy on outer orbitals of the adsorbed atom; $n_\sigma = a^+_\sigma a_\sigma$ is the operator of the number of electrons with the spin projection $\sigma$ at the device level; $a^+_\sigma$ is the electron creation operator, which creates an electron on the outer orbitals of the adsorbed atom with the spin projection $\sigma$; $U$ is the parameter characterizing the Hubbard repulsion of two electrons with opposite spin projections. The influence of the crystal environment on the magnetic properties of the adatom or an impurity is modeled by the uniaxial anisotropy parameter $D$. The effect of magnetic field on the energy structure of the impurity center with an effective $g$-factor is described by the Zeeman term in Eq. (3). The coupling between the spin degrees of freedom of a transported electron and the adatom occurs through the $s$–$d(f)$ exchange coupling and is described by the last term in Eq. (3), in which **S** is the vector operator of the spin moment of the atom, and **σ** is the vector operator of the spin of the transported electron. The parameter $A$ determines the intensity of the $s$–$d(f)$ exchange coupling.

The interaction of the three parts of the system described above is determined by the operator $\hat{T}$ defined in Eq. (1). This term takes into account the electron tunneling between the contacts and the device:

$$\hat{T} = \sum_{k\sigma} t_{Lk} c^+_{k\sigma} a_\sigma + \sum_{p\sigma} t_{Rp} d^+_{p\sigma} a_\sigma + \text{H.c.}, \tag{4}$$

where $t_{Lk}$, $t_{Rp}$ are the coupling parameters for the left and right contacts, respectively, and the adatom. The operator $\hat{V}_\varphi$ in the total Hamiltonian of the system is due to the bias voltage $V$ applied to the metal contacts:

$$\hat{V}_\varphi = \sum_\sigma (eV/2) a^+_\sigma a_\sigma + \sum_{p\sigma} (eV) d^+_{p\sigma} d_{p\sigma}. \tag{5}$$

### 3. The Hamiltonian of the multilevel structure in the atomic representation

As well known, the calculation of the transport characteristics of a magnetic adatom using the Keldysh technique involves construction of diagram series for the system of nonequilibrium Green's functions. The use of the Hamiltonian of the unperturbed system $\hat{H}_0$ ($\hat{H}_0 = \hat{H}_L + \hat{H}_R + \hat{H}_D$) in the representation of the second-quantization Fermi operators for this purpose complicates the process significantly due to the off-diagonal structure of the operator $\hat{H}_D$ in this representation. This problem can be overcome by writing the operator $\hat{H}_D$ in the atomic representation. To do this, the basis vectors of the Hilbert space of states are defined as the eigenvectors $|\psi_n\rangle$ of the device Hamiltonian $\hat{H}_D$, i.e., $\hat{H}_D|\psi_n\rangle = E_n|\psi_n\rangle$. Then the introduction of the Hubbard operators $X^{nm} = \langle\psi_n|\psi_m\rangle$ allows us to write the Hamiltonian of the magnetic adatom in a diagonal form:

$$\hat{H}_D = \sum_{n=1}^{12} E_n X^{nn}. \tag{6}$$

Let us provide the explicit form of the eigenvectors $|\psi_n\rangle$ and eigenenergies $E_n$ of the operator $\hat{H}_D$. The system under consideration has twelve levels ($n = 1,\ldots,12$). Three states have no electrons and differ by the spin projection of the adatom $S^z$:

$$|\psi_1\rangle = |0,0\rangle, \quad |\psi_{2,3}\rangle = |0,\pm 1\rangle. \tag{7}$$

Here and below ket-vectors in the right parts of the equations determine the state with a given number of electrons (first number) and the projection of the adatom spin (second number).

There are six states present in the one-electron spectrum

$$\begin{aligned}
|\psi_4\rangle &= \cos\Theta_+|\uparrow,0\rangle - \sin\Theta_+|\downarrow,+1\rangle,\\
|\psi_5\rangle &= \cos\Theta_-|\downarrow,0\rangle - \sin\Theta_-|\uparrow,-1\rangle,\\
|\psi_6\rangle &= \mathrm{sgn}(A)(\sin\Theta_+|\uparrow,0\rangle - \cos\Theta_+|\downarrow,+1\rangle),\\
|\psi_7\rangle &= \mathrm{sgn}(A)(\sin\Theta_-|\downarrow,0\rangle + \cos\Theta_-|\uparrow,-1\rangle),\\
|\psi_8\rangle &= |\uparrow,+1\rangle, \quad |\psi_9\rangle = |\downarrow,-1\rangle,
\end{aligned} \tag{8}$$

where the first index of a ket-vector shows the orientation of the spin of an electron located on the outer orbital of the adatom. The expansion coefficients are of the form

$$\begin{aligned}
&\sin\Theta_\pm = \mathrm{sgn}(A)\sqrt{\frac{1+x_\pm}{2}}, \quad \cos\Theta_\pm = \sqrt{\frac{1-x_\pm}{2}},\\
&x_\pm = \Delta_\pm/\nu_\pm, \quad \nu_\pm = \sqrt{\Delta_\pm^2 + A^2/2},\\
&\Delta_\pm = \Delta \pm \left(\frac{g}{2}-1\right)h, \quad \Delta = \frac{A}{4}-\frac{D}{2}, \quad h = \mu_B H.
\end{aligned} \tag{9}$$

The effect of a magnetic field is manifested through the dependence of these expressions on $h$. For real systems, in most cases, the conditions are satisfied under which the Zeeman interaction energy is less than the model parameters. Then in the linear approximation with respect to $h$, it is easy to establish an explicit dependence of the expansion coefficients on the magnetic field:

$$\begin{aligned}
&\sin\Theta_\pm \approx \sin\Theta \pm \left(\frac{g}{2}-1\right)h\frac{1-x}{2\nu}\sin\Theta,\\
&\cos\Theta_\pm \approx \cos\Theta \mp \left(\frac{g}{2}-1\right)h\frac{1+x}{2\nu}\cos\Theta,\\
&\sin\Theta = \mathrm{sgn}(A)\sqrt{\frac{1+x}{2}}, \quad \cos\Theta = \sqrt{\frac{1-x}{2}},\\
&x = \Delta/\nu, \quad \nu = \sqrt{\Delta^2 + A^2/2}.
\end{aligned} \tag{10}$$

The basis vectors of the two-electron sector are defined by the expressions

$$|\psi_1 0\rangle = |2,0\rangle, \quad |\psi_{11,12}\rangle = |2,\pm 1\rangle. \tag{11}$$

The eigenenergies $E_n$ of the device have the form:

$$\begin{aligned}
&E_1 = 0, \quad E_{2(3)} = D \mp gh, \quad E_{4(5)} = \xi_{d\uparrow(\downarrow)} - \Delta_\pm - \nu_\pm,\\
&E_{6(7)} = \xi_{d\uparrow(\downarrow)} - \Delta_\pm + \nu_\pm, \quad E_{8(9)} = \xi_{d\uparrow(\downarrow)} + D + A/2 \mp gh,\\
&E_{10} = 2\xi_d + U, \quad E_{11(12)} = 2\xi_d + U + D \mp gh.
\end{aligned} \tag{12}$$

As can be seen from the expression for the eigenenergies $E_n$ of an isolated device, in non-zero magnetic fields, there is a splitting of some levels which differ in the sign of the projection of the total spin $\sigma^z + S^z$. Consequently, we can expect to see more features in the CVCs, which are related to the Zeeman effect.

Let us introduce a representation of the Fermi operator $a_\sigma$ through the Hubbard operators:

$$\begin{aligned}
a_\sigma &= \sum_{n,m}\langle\psi_n|a_\sigma|\psi_m\rangle X^{n,m}\\
&\equiv \sum_{n,m}\gamma_\sigma(n,m)X^{n,m} \equiv \sum_\alpha \gamma_\sigma(\alpha)X^\alpha,
\end{aligned} \tag{13}$$

where $\gamma_\sigma(\alpha)$ are the parameters of the representation of the operator $a_\sigma$ through the Hubbard operators $X^\alpha$. For convenience of writing the following equations, the summation over two indices $(n, m)$ was changed to that over the root vector $\alpha(n, m)$.[23] Finding the parameters of the representation using Eqs. (7)–(11), we obtain:

$$\begin{aligned}
a_\uparrow &= [\mathrm{sgn}(A)X^{1,6} - X^{4,11}]\sin\Theta_+ + [X^{1,4} + \mathrm{sgn}(A)X^{6,11}]\cos\Theta_+\\
&\quad + X^{2,8} + [\mathrm{sgn}(A)X^{7,10} - X^{3,5}]\sin\Theta_-\\
&\quad + [X^{5,10} + \mathrm{sgn}(A)X^{3,7}]\cos\Theta_- + X^{9,12};\\
a_\downarrow &= -[X^{2,4} + \mathrm{sgn}(A)X^{6,10}]\sin\Theta_+\\
&\quad + [\mathrm{sgn}(A)X^{2,6} - X^{4,10}]\cos\Theta_+\\
&\quad + X^{3,9} + [\mathrm{sgn}(A)X^{1,7} + X^{5,12}]\sin\Theta_-\\
&\quad + [X^{1,5} - \mathrm{sgn}(A)X^{7,12}]\cos\Theta_- - X^{8,11}.
\end{aligned} \tag{14}$$

As can be seen from Eq. (14), in the system under study there are ten possible transitions where the number of electrons with the projection of spin $\sigma = +1/2$ is changed by unity. The same number of transitions are possible for electrons with $\sigma = -1/2$. The energies of the transitions for $\sigma = +1/2$ are (up to linear terms in $h$):

$$\begin{aligned}
&E_{1,4} = E_1 - E_4 \approx \Delta + \nu - \xi_d + g_+ h,\\
&E_{1,6} \approx \Delta - \nu - \xi_d + g_- h,\\
&E_{3,5} \approx \Delta + \nu + D - \xi_d + g_- h,\\
&E_{3,7} \approx \Delta - \nu + D - \xi_d + g_+ h,\\
&E_{2,8} = -(A/2 + \xi_d - h),\\
&E_{4,11} \approx -(\Delta + \nu + U + D + \xi_d) + g_- h,\\
&E_{5,10} \approx -(\Delta + \nu + U + \xi_d) + g_+ h,\\
&E_{6,11} \approx -(\Delta - \nu + U + D + \xi_d) + g_+ h,\\
&E_{7,10} \approx -(\Delta + \nu + U + \xi_d) + g_- h,\\
&E_{9,12} \approx -(U - A/2 + \xi_d - h),
\end{aligned} \tag{15}$$

where $g_\pm = g/2 \pm \frac{\Delta}{\nu}(g/2-1)$. The energies of the transitions for $\sigma = -1/2$ are written similarly.

#### 4. Expression for the current through a multilevel structure. Application of the atomic representation in the Keldysh technique

Application of an external electric bias $eV$ leads to non-equilibrium processes in the system. To obtain the diagrammatic form of the perturbation theory, let us perform a unitary transformation of the system Hamiltonian using the unitary operator[27]

$$\hat{U} = \exp\left(i\frac{eV}{2}t\sum_\sigma n_\sigma\right)\exp\left(ieVt\sum_{p\sigma} n_{p\sigma}\right).$$

The new tunneling operator has a time-dependent form now:

$$\begin{aligned}
\hat{T}_{\mathrm{eff}} &= \sum_{k\sigma,\alpha} t_k\gamma_\sigma(\alpha)[\mathrm{e}^{-ieVt/2}c_{k\sigma}^+ X^\alpha + \mathrm{e}^{ieVt/2}X^{-\alpha}c_{k\sigma}]\\
&\quad + \sum_{p\sigma,\alpha} t_p\gamma_\sigma(\alpha)[\mathrm{e}^{ieVt/2}c_{p\sigma}^+ X^\alpha + \mathrm{e}^{-ieVt/2}X^{-\alpha}c_{p\sigma}].
\end{aligned} \tag{16}$$

The expression for the electric current can be obtained from the ratio $I = e\langle dN_L/dt\rangle$. Then

$$\begin{aligned}
I = ie\sum_{k\sigma,\alpha} t_k\gamma_\alpha(\alpha)\Big[&\mathrm{e}^{\frac{ieV}{2}t}\langle\hat{T}_C X^{-\alpha}(t+\delta)c_{k\sigma}(t)S_C\rangle_0\\
&-\mathrm{e}^{-\frac{ieV}{2}t}\langle\hat{T}_C c_{k\sigma}^+(t+\delta)X^\alpha(t)S_C\rangle_0\Big],
\end{aligned} \tag{17}$$

where $\delta \to +0$;

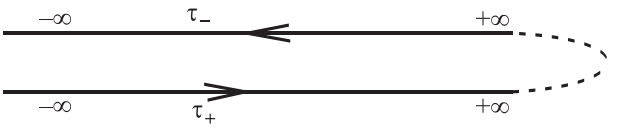


FIG. 2. Keldysh time-contour $C$.

$$\hat{T}_C, S_C = \sum_{n=0}^{\infty} \frac{(-i)^n}{n!} \int_C d\tau_1 \ldots d\tau_n \hat{T}_{eff}(\tau_1) \ldots \hat{T}_{eff}(\tau_n),$$

are the operators of $T$-ordering and evolution on the Keldysh contour $C$, respectively (see Fig. 2). The index 0 at the averages in Eq. (17) denotes averaging over the states of the unperturbed system. Equation (17) takes into account that upon the passage of current, when an electron propagates from the contact into the device, the latter changes its state, moving from one sector of the Hilbert space into another sector with an incremented or decremented number of electrons. There can be many transitions like that and all of them, generally, produce a non-zero contribution. This is accounted for by the summation over the variable $\alpha$ in Eq. (17). Here and below $\hbar = 1$.

The averages in Eq. (17) are expressed through the nonequilibrium mixed Green's functions:

$$G^{+-}_{k\sigma,\alpha}(t, t+\delta) = -i\langle \hat{T}_C c_{k\sigma}(t) X^{-\alpha}(t+\delta) S_C \rangle_0,$$
$$G^{+-}_{\alpha,k\sigma}(t, t+\delta) = -i\langle \hat{T}_C X^{\alpha}(t) c^{+}_{k\sigma}(t+\delta) S_C \rangle_0,$$

where time $t$ is located on the lower branch of the Keldysh contour $C$ ($t \in \tau_+$).[24] After expanding the evolution operator $S_C$, we obtain

$$G^{+-}_{k\sigma,\alpha}(t, t+\delta) = \sum_{\nu} t_k \gamma_\sigma(\nu) \int_C d\tau G_{k\sigma}(t-\tau) D_{\nu\alpha}(\tau - t - \delta),$$
$$G^{+-}_{\alpha,k\sigma}(t, t+\delta) = \sum_{\nu} t_k \gamma_\sigma(\nu) \int_C d\tau D_{\nu\sigma}(t+\delta-\tau) G_{k\alpha}(\tau - t), \tag{18}$$

where $G^{ab}_{k\sigma}(\tau - \tau')$ is the seed Green's function of the left contact. Its components after Fourier transformation have the form

$$\begin{aligned} G^{++}_{Lk\sigma}(\omega) &= \frac{n_{Lk\sigma}}{\omega - \xi_{Lk\sigma} - i\delta} + \frac{1 - n_{Lk\sigma}}{\omega - \xi_{Lk\sigma} + i\delta}, \\ G^{+-}_{Lk\sigma}(\omega) &= 2\pi i n_{Lk\sigma} \delta(\omega - \xi_{Lk\sigma}), \\ G^{--}_{Lk\sigma}(\omega) &= -\frac{n_{Lk\sigma}}{\omega - \xi_{Lk\sigma} + i\delta} - \frac{1 - n_{Lk\sigma}}{\omega - \xi_{Lk\sigma} - i\delta}, \\ G^{-+}_{Lk\sigma}(\omega) &= 2\pi i (n_{Lk\sigma} - 1) \delta(\omega - \xi_{Lk\sigma}). \end{aligned} \tag{19}$$

The function $D^{ab}_{\alpha\beta}$ in Eq. (18) is the complete Green's function of the magnetic adatom. Thus, after the Fourier transform, an intermediate expression for the current takes the form

$$I = e \sum_{k\sigma} t^2_{Lk} \int_{-\infty}^{+\infty} \frac{d\omega}{2\pi} \left[ G^{-+}_{Lk\sigma}(\omega) W^{+-}_{\sigma}\left(\omega - \frac{eV}{2}\right) \right]$$
$$- G^{+-}_{Lk\sigma}(\omega) W^{-+}_{\sigma}\left(\omega - \frac{eV}{2}\right), \tag{20}$$

where the spectral functions of the device are introduced

$$W^{ab}_{\sigma}(\omega) = \sum_{\alpha\beta} \gamma_\sigma(\alpha) \gamma_\sigma(\beta) D^{ab}_{\sigma\beta}(\omega).$$

Derivation of the equations for $D^{ab}_{\alpha\beta}$ is simplified if two factors are accounted for. The first is related to the fact that the operator $H_0$ is additive with respect to the subsystems of the two contacts and the device. Therefore, the average of the product of the Fermi and Hubbard operators can be decomposed into the product of the averages, each of which contains only the operators of one type. The second factor follows from the fact that the terms in the series for $D^{ab}_{\alpha\beta}(\tau - \tau')$, arising from the decomposition of the scattering matrix $S_C$, vanish as soon as the operator $\hat{T}_{\text{eff}}$ under the averaging sign appears an odd number of times. Moreover, in the terms of even order, the averages of the appearing products of Fermi operators are straightforward to calculate. As a result, the infinite series can be collapsed into an exponent so that the definition $D^{ab}_{\alpha\beta}$ includes a renormalized scattering matrix $\tilde{S}_C$:

$$D^{ab}_{\alpha\beta}(\tau - \tau') = -i\langle T_C X^{\alpha}(\tau_a) X^{-\beta}(\tau'_b) \tilde{S}_C \rangle_0, \tag{21}$$

which is determined through the effective interaction, which is related only to the device subsystem and is expressed using Hubbard operators

$$\tilde{S}_C = T_C \exp\left\{ -i \int_C d\tau_1 \int_C d\tau_2 \sum_{\alpha\beta} \tilde{V}_{\alpha\beta}(\tau_1 - \tau_2) X^{-\alpha}(\tau_1) X^{\beta}(\tau_2) \right\}. \tag{22}$$

It should be noted that a similar procedure has been used previously for obtaining the Green's functions of quasilocalized electrons in the Anderson model.[28]

The matrix elements of the effective interaction have the form:

$$\tilde{V}_{\alpha\beta}(\tau_1 - \tau_2) = \sum_{\sigma} \gamma_\sigma(\alpha) \gamma_\sigma(\beta) \left\{ \sum_k t^2_{Lk} e^{i\frac{eV}{2}(\tau_1 - \tau_2)} G_{Lk\sigma}(\tau_1 - \tau_2) \right.$$
$$\left. + \sum_p t^2_{Rp} e^{-i\frac{eV}{2}(\tau_1 - \tau_2)} G_{Rp\sigma}(\tau_1 - \tau_2) \right\}. \tag{23}$$

The carried out transformations show that for finding the nonequilibrium Green's functions $D^{ab}_{\alpha\beta}$ the diagrammatic technique for Hubbard operators,[22,23] modified in accordance with the Keldysh technique,[24] can be used. As a result, the equations can be written which take into account the contributions to $D^{ab}_{\alpha\beta}$ in all orders with respect to the coupling parameters for contacts $t_{Lk}$ and $t_{Rp}$. As a matter fact, this means that the problem of electron transport through a multilevel structure is solved, taking into account not only the processes of sequential tunneling, but also all possible processes of multiple inelastic cotunneling.

Fig. 3 shows in graphical form the system of equations for $D^{ab}_{\alpha\beta}(\omega)$ (double solid line). The solid lines denotes the seed functions $D^{ab}_{0\alpha}(\omega)$ which are given by the expressions

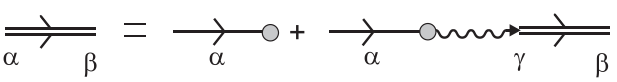


FIG. 3. Dyson equation for the Green's function $D^{ab}_{\alpha\beta}(\omega)$.

$$
\begin{aligned}
D_{0\alpha}^{++}(\omega) &= \frac{N_n}{\omega + E_\alpha + i\delta} + \frac{N_m}{\omega + E_\alpha - i\delta},\\
D_{0\alpha}^{+-}(\omega) &= 2\pi i N_m \delta(\omega + E_\alpha),\\
D_{0,\alpha}^{--}(\omega) &= -\frac{N_n}{\omega + E_\alpha - i\delta} - \frac{N_m}{\omega + E_\alpha + i\delta},\\
D_{0\alpha}^{-+}(\omega) &= -2\pi i N_m \delta(\omega + E_\alpha).
\end{aligned}
\tag{24}
$$

The quantity $E_\alpha$ denotes the difference between the energy levels $n$ and $m$, i.e., $E_\alpha = E_n - E_m$ for $\alpha = \alpha(n, m)$. It is important to note that the occupation numbers of the eigenstates of the adatom, $N_n$ and $N_m$, in the expressions for $D_{0\alpha}^{ab}(\omega)$ are non-equilibrium, i.e., depend on both the coupling with contacts and the applied bias. This is reflected in Fig. 3 as circles. The wavy line corresponds to the Fourier transform of the effective interaction, Eq. (23)

$$
\tilde{V}_{\alpha\beta}^{ab}(\omega) = \sum_\sigma \gamma_\sigma(\alpha)\gamma_\sigma(\beta) M_\sigma^{ab}(\omega),
\tag{25}
$$

where

$$
M_\sigma^{ab}(\omega) = \sum_k t_{Lk}^2 G_{Lk\sigma}^{ab}\left(\omega + \frac{eV}{2}\right) + \sum_p t_{Rp}^2 G_{Rp\sigma}^{ab}\left(\omega - \frac{eV}{2}\right).
\tag{26}
$$

As can be seen from Eq. (25), the dependence of the matrix interaction elements on the root vectors $\alpha$ and $\beta$ has the split character. This allows us to apply the approach of Ref. 29 for solving the system of Dyson equations by the Keldysh technique.[24] Thus, we find

$$
W_\sigma^{+-}(\omega) = -\frac{M_\sigma^{+-}(\omega)}{\Delta_\sigma(\omega)}, \quad W_\sigma^{-+}(\omega) = -\frac{M_\sigma^{-+}(\omega)}{\Delta_\sigma(\omega)},
\tag{27}
$$

where

$$
\begin{aligned}
\Delta_\sigma(\omega) = &\left\{\left[\sum_\alpha \gamma_\alpha^2(\alpha) D_{0\alpha}^{++}(\omega)\right]^{-1} - M_\sigma^{++}(\omega)\right\}\\
&\times \left\{\left[\sum_\alpha \gamma_\sigma^2(\alpha) D_{0\alpha}^{--}(\omega)\right]^{-1}\right.\\
&\left. - M_\sigma^{--}(\omega)\right\} - M_\sigma^{+-}(\omega) M_\sigma^{-+}(\omega).
\end{aligned}
\tag{28}
$$

As a result, the general expression for the current through a multilevel structure is written as follows:

$$
\begin{aligned}
I_L = 2e \sum_\sigma \int_{-\infty}^{+\infty} \frac{d\omega}{\pi} &\left[n(\omega - eV) - n(\omega)\right]\\
&\times \frac{\Gamma_{L\sigma}(\omega)\Gamma_{R\sigma}(\omega)}{\left[L_\sigma^{-1}(\omega) - \Lambda_\sigma(\omega)\right]^2 + \Gamma_\sigma^2(\omega)},
\end{aligned}
\tag{29}
$$

where

$$
\begin{aligned}
L_\sigma(\omega) &= \sum_\alpha \frac{b_\alpha \gamma_\sigma^2(\alpha)}{\omega + E_\alpha - eV/2},\\
\Lambda_\sigma &= \sum_k \frac{t_{Lk}^2}{\omega - \xi_{Lk\sigma}} + \sum_p \frac{t_{Rp}^2}{\omega - \xi_{Rp\sigma} - eV}.
\end{aligned}
\tag{30}
$$

Obtained Eq. (29) is proportional to the product $t_L^2 t_R^2$ and satisfies the symmetry requirements.[30] In this paper, as already noted, the approximation of wide-band metal contacts is used for the actual calculations. Later on, this will allow us to neglect both the shift $\Lambda_\sigma$ and the frequency dependence of the level broadening functions $\Gamma_\sigma = \Gamma_{L\sigma} + \Gamma_{R\sigma} = \pi(t_L^2 g_{L\sigma} + t_R^2 g_{R\sigma})$, where $t_{L(R)}$ is the parameter of electron hopping from the last node of the left (right) contact to the level of the magnetic adatom; $g_{L(R)\sigma}$ is the spin-dependent density of states of the left (right) contact.[31] For simplicity, in the numerical calculations we assume $g_{L(R)\sigma} = 1/W$ as $W \gg h$.

As was noted above when discussing the Dyson equation, the occupation numbers in this system are nonequilibrium, and their dependence on the electric bias is determined by solving the system of quantum kinetic equations with the condition $\sum_{i=1}^{12} N_i = 1$,

$$
\begin{aligned}
N_m = \frac{1}{2\pi i}\int_{-\infty}^{+\infty} d\omega D_{\alpha\alpha}^{+-}(\omega) = \int_{-\infty}^{+\infty} \frac{d\omega}{\pi} &\frac{b_\alpha^2 \gamma_\sigma^2(\alpha)}{(\omega + E_\alpha - eV/2)^2}\\
&\times \frac{\Gamma_{L\sigma}(\omega) n(\omega) + \Gamma_{R\sigma}(\omega) n(\omega - eV)}{\left[1 - \Lambda_\sigma(\omega) L_\sigma(\omega)\right]^2 + \Gamma_\sigma^2(\omega) L_\sigma^2(\omega)}.
\end{aligned}
\tag{31}
$$

Equation (31) does not include a summation over the spin variable. This is due to the fact that the magnetic field and the anisotropy axis are collinear. Therefore, for each single-fermion transition $\alpha = \alpha(n, m)$, out of two presentation parameters, $\gamma_\uparrow(\alpha)$ and $\gamma_\downarrow(\alpha)$, only one is different from zero.

In carrying out numerical calculations let us take into account that experimentally at low temperatures, the regime of weak (tunnel) coupling between the magnetic adatom and contacts is most often realized.[7,8] Mathematically this is expressed as smallness of the temperature and the energy levels broadening as compared to the distance between these levels: $T, \Gamma_\sigma \ll E_\alpha$. Taking into account the above relations we obtain

$$
\begin{aligned}
N_m \simeq \frac{b_\alpha}{\pi}\left[\frac{\pi}{2} + \frac{\Gamma_{L\sigma}}{\Gamma_\sigma}\arctan\left(\frac{\omega_{0\alpha} - eV/2}{\kappa_\alpha}\right)\right.\\
\left. + \frac{\Gamma_{R\sigma}}{\Gamma_\sigma}\arctan\left(\frac{\omega_{0\alpha} + eV/2}{\kappa_\alpha}\right)\right],
\end{aligned}
$$

where

$$
\omega_{0\alpha} = E_\alpha + \lambda_\alpha \kappa_\alpha, \quad \kappa_\alpha = \frac{b_\alpha \gamma_\sigma^2(\alpha)\Gamma_\sigma}{1 + \lambda_\alpha^2}, \quad \lambda_\alpha = \sum_{\beta \neq \alpha} \frac{b_\beta \gamma_\sigma^2(\beta)\Gamma_\sigma}{E_\beta - E_\alpha}.
$$

In this mode, the main contribution to the tunneling current comes from the diagonal terms $I \simeq \sum_\alpha I_{\alpha\alpha}$ so

$$
\begin{aligned}
I \simeq \frac{2e}{\pi}\frac{\Gamma_{L\sigma}\Gamma_{R\sigma}}{\Gamma_\sigma}\sum_\alpha b_\alpha \gamma_\sigma^2(\alpha)\\
\times \left[\arctan\left(\frac{\omega_{0\alpha} + eV/2}{\kappa_\alpha}\right) - \arctan\left(\frac{\omega_{0\alpha} - eV/2}{\kappa_\alpha}\right)\right].
\end{aligned}
\tag{32}
$$

### 5. Analysis of the results

Figure 4 shows the dependence of the non-equilibrium occupation numbers $N_i(eV)$ $(i = 1,\ldots,12)$ in the system "magnetic adatom + electrons" on the electric field in the

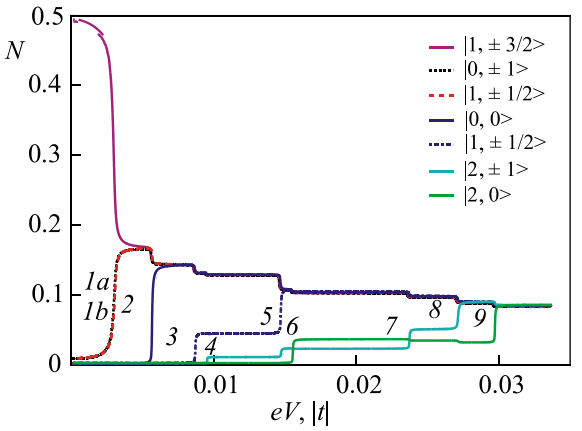


FIG. 4. Dependence of the nonequilibrium occupation numbers on the energy of an electric field, plotted for $t_L = t_R = t/100$, $\varepsilon_d = 0.001|t|$, $A = -0.005|t|$, $U = 0.01|t|$, $D = -0.003|t|$, $T = 0.1$ K, $h = 0$.

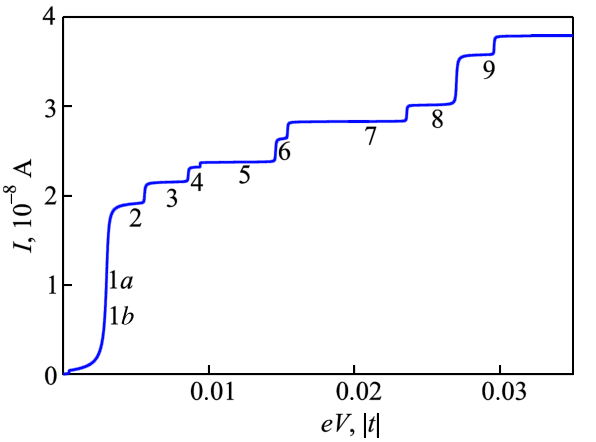


FIG. 6. Current-voltage characteristic of a magnetic adatom, plotted for the parameters of Fig. 4.

tunneling regime at low temperatures. It can be seen that the $N_i(eV)$ behave similarly: an increase in voltage is accompanied by alternating steps, when $N_i$ undergo significant changes, and plateaus, where these changes are negligible. Moreover, each step corresponds to activation of the corresponding transition, as can be seen from the comparison of Fig. 4 with the schematics of possible transitions, shown in Fig. 5. For the selected parameters, which are of the same order of magnitude as those obtained in experiments[15] and used in numerical calculations,[32,33] the ground state of the device is the single-fermion spin doublet with the projection of the total spin $\pm 3/2$ (states $|\psi_{8,9}\rangle = |1, \pm 3/2\rangle$). As a consequence, $N_{8,9}(eV \approx 0) \approx 0.5$ in Fig. 4 (purple solid curve). The fact that the probabilities $N_{8,9}$ differ from 1/2 and also the residual population of other states are a direct consequence of the non-equilibrium character of the system. With increasing energy of the electric bias field, there is an increase in the energy of an electron tunneling to the outer orbitals of the adatom. As a result, transitions into the excited states become available. First, two zero-electron states with $S^z = \pm 1$, $N_{2,3}$ (black dotted line) become occupied, and the occupation numbers $N_{8,9}$ are reduced. The corresponding sharp change in the population is marked as *1a*. The actual transition in Fig. 5 has the same index. As seen in Fig. 4, together with an increase in the occupation number $N_{2,3}$, there is also an increase in the numbers $N_{4,5}$ (dashed curve 2), which describe the one-electron states with $\sigma^z + S^z = \pm 1/2$ and have an antisymmetric wave function Eq. (8). This is due to the fact that $E_{3,5}(E_{2,4}) < E_{2,8}$ $(E_{3,9})$, and, because the numbers $N_{2,3}$ are very small for $eV/2 < E_{2,8}$ $(E_{3,9})$, the transition denoted as *1b* does not occur for these voltages. In accordance with the above, it is expected that each transition induces a corresponding sharp change in the population of the system levels.

Fig. 6 shows the CVC of a magnetic adatom in the regime of tunnel coupling at low temperatures. Since the current $I_{\alpha\alpha}$ in the channel $\alpha$ depends on the occupation numbers [see Eq. (32)], the specific features similar to those discussed above also appear in the CVC. The observed dependence is well known and is a sequence of the Coulomb steps.[7,8] Each step corresponds to the appearance of a new current channel, the contribution of which to the total current $I_{\alpha\alpha}$ is $2e\Gamma_{L\sigma}\Gamma_{R\sigma}b_\alpha\gamma^2_\sigma(\alpha)/\Gamma_\sigma$.

Zeeman splitting of the levels in the system in nonzero magnetic fields causes the appearance of additional Coulomb steps in the CVC upon switching on a magnetic field (curve *1* in Fig. 7). Especially interesting is the fact that for $h \neq 0$, regions with negative differential conductivity (NDC), $dG/dV < 0$ [dashed line in Fig. 8(a)], appear in the CVC.[7,8] A drop in current with increasing voltage in this

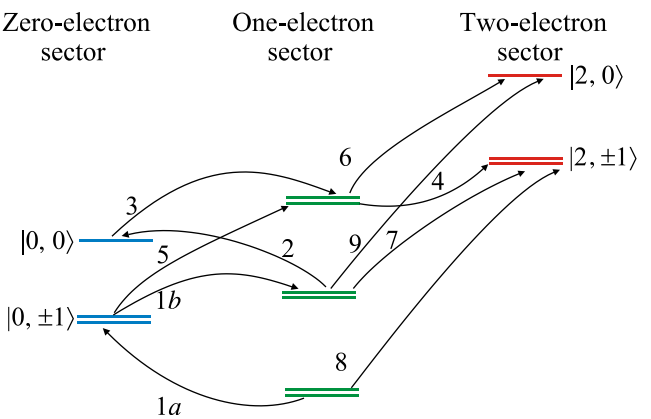


FIG. 5. Energy spectrum and possible electronic transitions between the levels of the system, drawn for the parameters of Fig. 4.

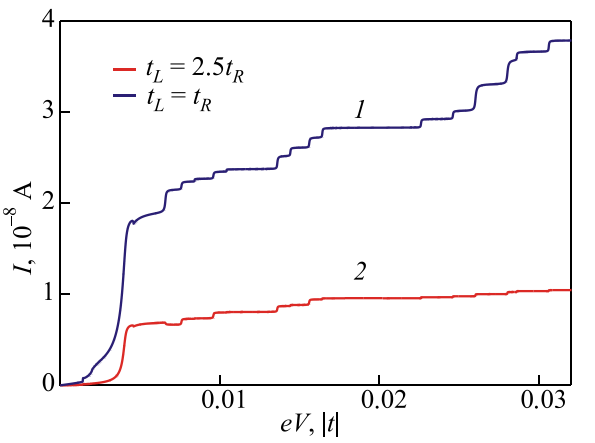


FIG. 7. Effect of a magnetic field on the current-voltage characteristics for symmetrical and asymmetrical coupling with the contacts, plotted for the parameters of Fig. 4 with $h = 5 \times 10^{-4}|t|$ and $g = 2$.

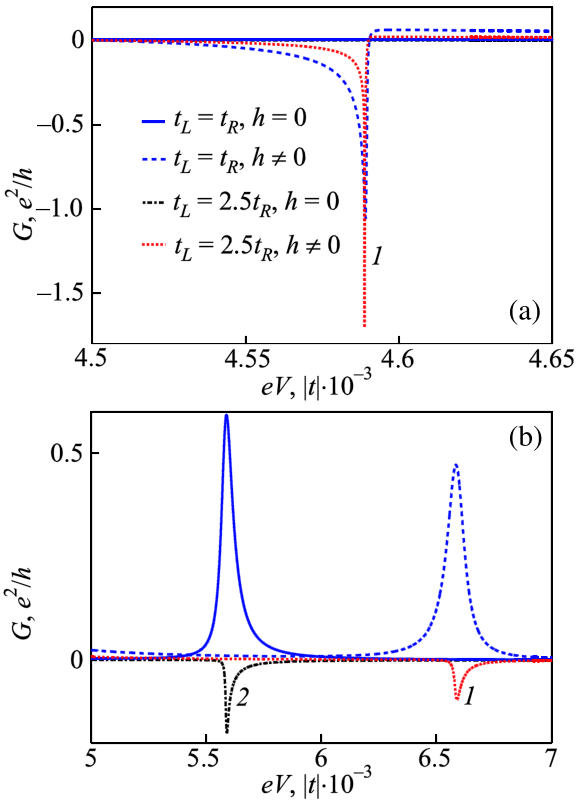


FIG. 8. Negative differential conductance (NDC) induced by a magnetic field (a); NDC due to the asymmetry of the adatom coupling with the contacts (b) (parameters taken from Fig. 7).

system is due to the processes of multiple inelastic scattering, which lead to the appearance of transitions from excited states to even higher lying states. In this case a situation may be realized when the contribution of a new channel $I_{\alpha\alpha}$ to the total current $I$ is small due to smallness of the factor $b_\alpha \gamma_\sigma^2(\alpha)$. Therefore, the extra current that appears is insufficient to compensate for the current reduction in other channels. An important role is played here by an additional non-linear factor, which depends on the condition of completeness: $\sum_{i=1}^{12} N_i = 1$.

Previously, it has been shown that the NDC of a magnetic adatom arising upon a change in the anisotropy parameter $D$ increases when the coupling between the structure and the contacts becomes asymmetric.[25,26] A similar pattern is observed in the case of the feature induced by a magnetic field [red dotted line 1 in Fig. 8(a)]. On the other hand, the magnetic field can also act as a mechanism of attenuating the NDC. As can be seen in Fig. 8(b), the conductivity minimum, which appears for $t_L \neq t_R$ (black dot-dashed line, *2*), moves higher for $h \neq 0$ (red dotted line *1*).

### 6. Conclusion

This paper presents the development of the theory of quantum transport through a multilevel structure, adsorbed inside a break junction between paramagnetic metal electrodes in nonzero magnetic fields at finite temperatures. An important aspect of this study is that the effects of multiple inelastic scattering of conduction electrons by a magnetic adatom under non-equilibrium conditions were accounted for. As a result of the above processes, the excited states of the system "magnetic adatom + electrons" become included in quantum transport. Moreover, allowing for the effects of multiple scattering makes possible the subsequent transitions from excited states to higher lying energy states.[11] When constructing the perturbation theory for systems with multiple interactions and a large set of nonequidistant transitions between levels, the atomic representation was used. Through the application of the Keldysh diagrammatic technique, constructed also using the Hubbard operators, it was shown that the CVC of a magnetic atomic structure in the tunneling regime at low temperatures exhibits typical features of the Coulomb blockade phenomenon in the form of steps. The effect of a magnetic field on the system is also manifested by lifting the degeneracy in energy for the transitions of electrons with spin $+1/2$ and $-1/2$. This in turn leads to an increase in the number of the Coulomb steps in the CVC. It was found that the magnetic field can both induce the NDC on an adatom and suppress this effect. The origin of the NDC, which is also observed in experiments,[7,8] is due to allowing for the multiple inelastic scattering and the coherent behavior of nonequilibrium occupation numbers of the system, determined by the condition of completeness. It was also noted that in practice the NDC can be enhanced by asymmetric coupling to the contacts.

This work was supported by the Program of the Presidium of RAS "Quantum mesoscopic and disordered systems" and Russian Foundation for Basic Research (Grant Nos. 13-02-00523, 13-02-98013, and 14-02-31280).

One of the authors (S.V.A.) is grateful to the grant of the President of the Russian Federation MK-526.2013.2 and the scholarship of the President of the Russian Federation SP-6361.2013.5 for the support.

[a]Email: vvv@iph.krasn.ru
[b]Email: asv86@iph.krasn.ru

[1]D. Gatteschi, R. Sessoli, and J. Villain, *Molecular Nanomagnets* (Oxford University Press, Oxford, 2006).
[2]J. M. Seminario, *Molecular and Nanoelectronics: Analysis, Design and Simulation* (Elsevier, Oxford, 2007).
[3]P. I. Arseyev, N. S. Maslova, and V. N. Mantsevich, Zh. Eksp. Teor. Fiz. **142**, 156 (2012) [JETP **115**, 141 (2012)].
[4]K. Kikoin and Y. Avishai, Phys. Rev. Lett. **86**, 2090 (2001).
[5]H. Ueba, T. Mii, and S. G. Tikhodeev, Surf. Sci. **601**, 5220 (2007).
[6]J. J. Park, A. N. Pasupathy, J. I. Goldsmith, C. Chang, Y. Yaish, J. R. Petta, M. Rinkoski, J. P. Sethna, H. D. Abruna, P. L. McEuen, and D. C. Ralph, Nature **417**, 722 (2002).
[7]H. B. Heersche, Z. de Groot, J. A. Folk, H. S. J. van der Zant, C. Romeike, M. R. Wegewijs, L. Zobbi, D. Barreca, E. Tondello, and A. Cornia, Phys. Rev. Lett. **96**, 206801 (2006).
[8]M.-H. Jo, J. E. Grose, K. Baheti, M. M. Deshmukh, J. J. Sokol, E. M. Rumberger, D. N. Hendrickson, J. R. Long, H. Park, and D. C. Ralph, Nano Lett. **6**, 2014 (2006).
[9]A. J. Heinrich, J. A. Gupta, and C. P. Lutz, Science **306**, 466 (2004).
[10]C. F. Hirjibehedin, C. P. Lutz, and A. J. Heinrich, Science **312**, 1021 (2006).
[11]S. Loth, K. von Bergmann, M. Ternes, A. F. Otte, C. P. Lutz, and A. J. Heinrich, Nat. Phys. **6**, 340 (2010).
[12]A. Bellec, L. Chaput, G. Dujardin, D. Riedel, L. Stauffer, and P. Sonnet, Phys. Rev. B **88**, 241406(R) (2013).
[13]S. Loth, S. Baumann, C. P. Lutz, D. M. Eigler, and A. J. Heinrich, Science **335**, 196 (2012).
[14]R.-N. Wang, J. H. Rodriguez, and W.-M. Liu, Phys. Rev. B **89**, 235414 (2014).

[15]C. F. Hirjibehedin, C.-Y. Lin, A. F. Otte, M. Ternes, C. P. Lutz, B. A. Jones, and A. J. Heinrich, Science **317**, 1199 (2007).
[16]N. Tsukahara, K.-I. Noto, M. Ohara, S. Shiraki, N. Takagi, Y. Takata, J. Miyawaki, M. Taguchi, A. Chainani, S. Shin, and M. Kawai, Phys. Rev. Lett. **102**, 167203 (2009).
[17]P. Ruiz-Diaz, R. Garibay-Alonso, J. Dorantes-Davila, and G. M. Pastor, Phys. Rev. B **84**, 024431 (2011).
[18]S. Bornemann, O. Sipr, S. Mankovsky, S. Polesya, J. B. Staunton, W. Wurth, H. Ebert, and J. Minar, Phys. Rev. B **86**, 104436 (2012).
[19]O. Sipr, S. Bornemann, H. Ebert, S. Mankovsky, J. Vackar, and J. Minar, Phys. Rev. B **88**, 064411 (2013).
[20]A. F. Otte, M. Ternes, K. von Bergmann, S. Loth, H. Brune, C. P. Lutz, C. F. Hirjibehedin, and A. J. Heinrich, Nat. Phys. **4**, 847 (2008).
[21]J. J. Park, A. R. Champagne, T. A. Costi, W. W. Shum, A. N. Pasupathy, E. Neuscamman, S. Flores-Torres, P. S. Cornaglia, A. A. Aligia, C. A. Balseiro, G. K.-L. Chan, H. D. Abruna, and D. C. Ralph, Science **328**, 1370 (2010).
[22]R. O. Zaitsev, Zh. Eksp. Teor. Fiz. **68**, 207 (1975) [Sov. Phys. JETP **41**, 100 (1975)].
[23]R. O. Zaitsev, Zh. Eksp. Teor. Fiz. **70**, 1100 (1976) [Sov. Phys. JETP **43**, 574 (1976)].
[24]L. V. Keldysh, Zh. Eksp. Teor. Fiz. **47**, 1515 (1964) [Sov. Phys. JETP **20**, 1018 (1965)].
[25]V. V. Val'kov, S. V. Aksenov, and E. A. Ulanov, Pis'ma Zh. Eksp. Teor. Fiz. **98**, 459 (2013) [JETP Lett. **98**, 403 (2013)].
[26]V. V. Val'kov, S. V. Aksenov, and E. A. Ulanov, Zh. Eksp. Teor. Fiz. **146**, 144 (2014) [JETP **119**, 124 (2014)].
[27]R. O. Zaitsev, *Introduction to Modern Kinetic Theory: A Lecture Course* (KomKniga, Moscow, 2007) (in Russian).
[28]V. V. Val'kov and D. M. Dzebisashvili, Zh. Eksp. Teor. Fiz. **134**, 791 (2008) [JETP **107**, 679 (2008)].
[29]V. V. Val'kov and T. A. Val'kova, Fiz. Nizk. Temp. **11**, 951 (1985) [Sov. J. Low Temp. Phys. **11**, 524 (1985)].
[30]P. I. Arseyev and N. S. Maslova, Usp. Fiz. Nauk **180**, 1197 (2010) [Phys.-Usp. **53**, 1151 (2010)].
[31]S. G. Tikhodeev and H. Ueba, in *Problems of Condensed Matter Physics*, edited by A. L. Ivanov and S. G. Tikhodeev (Clarendon Press, Oxford, 2008).
[32]K. Park and M. R. Pederson, Phys. Rev. B **70**, 054414 (2004).
[33]F. Qu and P. Hawrylak, Phys. Rev. Lett. **95**, 217206 (2005).

Translated by L. Gardt